THE JOURNAL OF PHYSICAL CHEMISTRY C
A JOURNAL OF THE AMERICAN CHEMICAL SOCIETY

pubs.acs.org/JPCC

Article

# The Role of Speed in Atomic Scale Wear

Shivaranjan Raghuraman, Perawat Boonpuek, Kyle H. King, Zhijiang Ye, and Jonathan R. Felts*

Cite This: *J. Phys. Chem. C* 2021, 125, 4139–4145

Read Online

ACCESS | Metrics & More | Article Recommendations | Supporting Information

**ABSTRACT:** Decoupling the role of various stress components during atomic scale wear—such as normal, shear, and hoop stresses—remains one of the biggest challenges preventing a full understanding of how wear proceeds. Here we model atomic scale wear as two sets of thermally activated processes, where normal load drives bonding between surfaces, and lateral motion biases surface site hopping in the direction of sliding. We further utilize the model to explain the velocity-dependent wear behavior at the interface between an atomic force microscope tip and graphene oxide. The experimental and theoretical results show that, at tip speeds slow enough to saturate bond formation at the tip−sample interface, breaking these bonds is a thermally activated process with a rate that increases with speed. In addition, the theoretical model predicts additional wear dependencies on velocity also observed in the literature, where a decrease in wear with increasing velocity occurs when the tip moves too quickly for bonds to form on the surface, and wear independent of velocity occurs at high loads when the thermodynamic barrier to wear is vanishingly small. This theoretical framework potentially unifies the range of velocity-dependent wear behaviors found in previous studies of atomic scale wear.

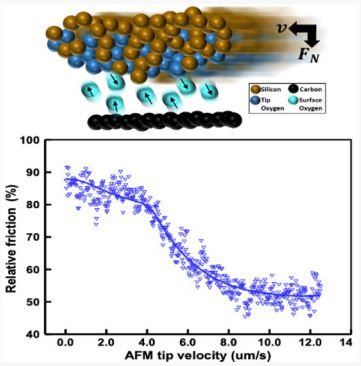




## 1. INTRODUCTION

Nearly one-quarter of worldwide energy consumption is due to losses in tribological contacts.[1,2] Understanding mechanical wear—the destructive attrition of surfaces in solid sliding contacts—is critical to improving energy efficiency. Historically, wear has been treated largely phenomenologically, interpreted by using the Archard wear equation $Q \propto F_N L/H$ where $Q$ is the wear volume, $F_N$ is the applied normal load, $L$ is the sliding distance, and $H$ is the hardness of the softest surface.[3,4] While this empirical observation holds remarkably well at the macroscale, the relationship breaks down in nanoscale contacts under low applied load, in which wear can be described as an activated atomic attrition process.[5,6] Although the exponential dependence of atomic scale wear on applied normal stress has become largely accepted within the tribology community, it remains unclear how the applied contact stress and the motion of the sliding interface work in concert to drive wear.

In contrast to atomic wear, studies of atomic scale friction have flourished in the past decade to include effects from atomic energy corrugation,[7−9] contact aging via covalent bonding,[10,11] chemically reactive lubricants,[12] and geometric effects such as the layer-dependent screening of long-range forces and Moiré pattern effects in stacked 2D materials[13] as well as atomic rearrangement at the contact interface. In all of these cases, the roles of normal and shear stresses on the contact mechanics are fairly clear: (1) normal stress contributes to friction by increasing contact area, increasing surface energy corrugation, and mechanically activating chemical bonding within the contact, and (2) shear stress is the byproduct of attempting to overcome long-range forces, hopping the energy corrugation barrier, and breaking interfacial bonds.

While it is known that larger normal stresses increase atomic-scale wear, it is currently unclear what role shear stress plays during this process, as it is difficult to decouple increases in shear stress from increases in normal stress. A number of velocity-dependent wear theories have been proposed, decomposing wear into two fundamental components: (1) an interaction between contacting surfaces (either mechanical or chemical) and (2) lateral transport of mass. If both of these are thermally activated processes, then there should exist a range of sliding conditions in which wear is exponentially dependent on both applied contact load and sliding velocity. Depending on the relative magnitude of each barrier, a number of velocity-dependent behaviors can result. For wear rates limited by the time required to form bonds within the contact, the rate should decrease with increasing velocity, as the atoms on the contacting surfaces have less time to interact. This behavior is the most commonly observed behavior for atomic scale wear, making it difficult to understand the role of lateral forces, as it is precisely in this limit that lateral forces are insignificant.[14−18] In contrast, if lateral transport of mass is the rate-limiting thermally activated barrier, one would expect the wear rate to increase with increasing velocity, in a manner similar to atomic-scale friction. There are a few experiments that have shown increasing wear with increasing velocity, although the effect of velocity on wear

**Received:** October 9, 2020
**Revised:** January 15, 2021
**Published:** February 16, 2021

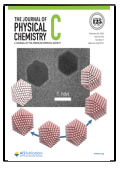




https://dx.doi.org/10.1021/acs.jpcc.0c09191
*J. Phys. Chem. C* 2021, 125, 4139−4145

was explained by using different mechanisms, such as a logarithmic dependence on sliding speed or exponential with velocity due to flash heating in the contact.[19,20]

Here we show through combined theory and experiment that wear of a single layer of oxygen molecules on graphene under a sliding silicon nanoasperity is activated by both normal stress and lateral motion (Figure 1). Our previous experiments on the

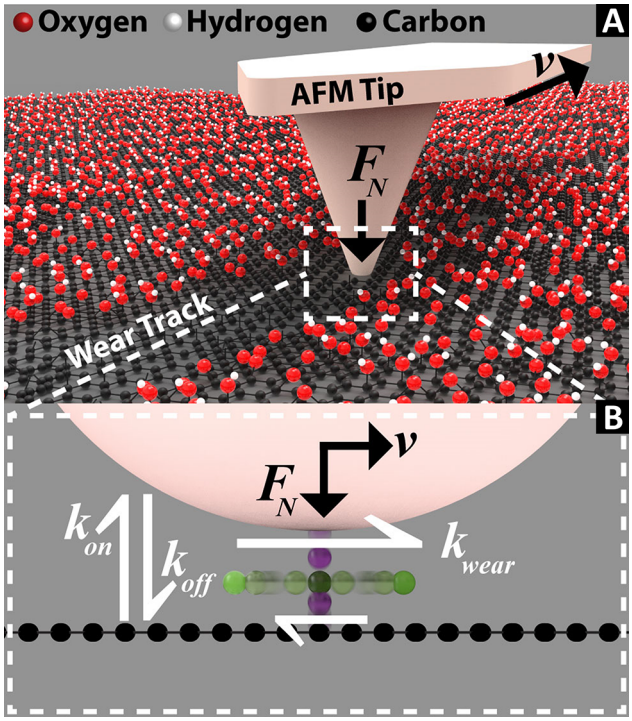


**Figure 1.** (A) Schematic of the experiment, where the nanoscale asperity of an atomic force microscope probe slides over graphene oxide, mechanically removing oxygen groups during sliding. (B) Theoretical dynamic picture of atomic scale wear, in which normal load affects the rate of bonding and unbonding at the contact interface and velocity biases thermally activated surface diffusion to produce a net lateral diffusion of wear species on the surface.

mechanochemical removal of oxygen groups from graphene oxide focused on the role of normal load and applied temperature.[21,22] In this study, the primary focus is the effect of tip velocity, and therefore lateral load, on the wear rate of the oxygen groups. We propose a kinetic model of wear, in which surface species must first bond to the tip before wear initiation, where the bonding and unbonding rates—and therefore the time that an interfacial bond persists—are modulated by applied normal load (higher normal loads lead to longer bond lifetimes). During the lifetime of the bond, the motion of the tip does work to overcome the surface forces holding the wear species in place and cause lateral motion across the surface. Because the work performed on the bond over the bond lifetime is proportional to velocity, higher velocities produce larger wear rates. Extrapolating the results determined here to a wide range of velocities and forces predict previously identified wear processes as high force and high speed limits to the general theory of thermally activated atomic scale wear.

## 2. MATERIALS AND METHODS

**2.1. Theoretical Treatment of Mechanochemical Wear.** In general, wear can be modeled as three thermally activated processes: bonding, unbonding, and lateral hopping between surface sites. Specifically, the bonding process occurs when an oxygen group on the graphene surface chemically interacts with the tip, where the unbonding process is the reverse of bonding, in which the oxygen group returns back to interacting only with the graphene substrate. The removal of oxygen species from the graphene surface is dictated by the number of species bound to the moving tip and the speed of the moving tip. The concentration of species attached to the tip is determined by the relative rates of bonding and unbonding, given by

$$k_{on} = k_0 e^{-[(E_{on} - \frac{1}{2}P(\vec{r},t)\Delta V_1)/k_b T]} \quad (1)$$

$$k_{off} = k_0 e^{-[(E_{off} + \frac{1}{2}P(\vec{r},t)\Delta V_1)/k_b T]} \quad (2)$$

where $k_{on}$ is the bonding rate, $k_{off}$ is the unbonding rate, $k_0$ is an attempt frequency, $E_{on}$ is the energy barrier for bonding, $E_{off}$ is the energy barrier for unbonding, $P(\vec{r},t)$ is the local pressure within the tip contact, $\Delta V_1$ is the change in activation volume between bound and activated states, $k_b$ is Boltzmann's constant, and $T$ is the local temperature. The pressure distribution at a specific location on the surface along the sliding tip pathway is a function of both the distance from the tip and time because of contact area overlap during continuous sliding. More specifically, when the tip contact area initially reaches the point of interest, the pressure at that time is zero and follows a parabolic trajectory as the tip passes over it. Therefore, $P(\vec{r},t)$ is given by an axisymmetric radial pressure distribution in the asperity contact that slides over the location at a constant velocity $U$

$$P(\vec{r}, t) = P_0\left(1 - \frac{(a - Ut)^2}{a^2}\right)^{-1/2}\left(1 - \frac{r^2}{2aUt - (Ut)^2}\right)^{-1/2} \quad (3)$$

where $P_0$ is the maximum pressure at the center of the contact and $a$ is the radius of the contact area between the asperity and the surface. The values of $P_0$ and $a$ are given by eqs 4−6 using Hertz contact mechanics

$$P_0 = \frac{3F_n}{2\pi a^2} \quad (4)$$

$$a = \left(\frac{3F_n R}{4E_s}\right)^{1/3} \quad (5)$$

$$E_s = \left[\frac{1 - \nu_1}{E_1} + \frac{1 - \nu_2}{E_2}\right]^{-1} \quad (6)$$

where $F_n$ is the applied load and $E_s$ is the effective elastic modulus of the interface calculated by using Poisson's ratio $\nu$ and the elastic modulus $E$ for both the tip and the substrate materials. The Hertz contact model assumes there is no adhesion between the surfaces, and while there is significant adhesion measured in our experiments, adhesion is ignored in our model for the following reasons. First, we assume that individual chemical bonds that are formed in the contact are in time-averaged equilibrium with its surrounding environment (that is, in the absence of external load, the bond cannot perform mechanical work on the tip or substrate). Second, existing adhesion models primarily rely on purely attractive forces, while in our case here we observe a significant energy barrier (repulsive interaction) to bond formation. Depending on the exact shape of the potential


https://dx.doi.org/10.1021/acs.jpcc.0c09191
J. Phys. Chem. C 2021, 125, 4139−4145

energy surface of this reaction, this could lead to a net increase, decrease, or no change in contact pressure. It remains an open question as to what effect adhesion has on the contact area and pressure distribution at the tip interface, although our observation that the wear rate is strongly dependent on compressive normal load suggests that the vast majority of the reactions are occurring near the center of the contact, and any net attraction at the perimeter is unlikely to be the dominant driving mechanism here. Therefore, the Hertzian approximation provides a reasonable relationship between applied normal force and wear. Additionally, the contact area, and therefore dwell time, depends on the tip radius of the AFM probe used, which we estimate based on the width of our wear tracks to be ∼100 nm. The wear rate is also modeled as an activated process

$$k_w = 2k_0 e^{-[E_w/k_bT]} \sinh \frac{sU\tau\lambda}{2k_bT} \tag{7}$$

where $E_w$ is a function of $P(\vec{r},t)$ and is the energy barrier for a bonded species to hop surface sites (which can also be a function of applied pressure), $s$ represents the spring constant resisting wear molecules hopping over the energy barrier (or the inverse of the curvature of the potential energy well), $\lambda$ = 1.4 Å is the distance between carbon atoms in the graphene lattice (the smallest discrete distance a surface species can travel), and $\tau = 1/k_{off}$ is the average lifetime of a bond. In the absence of sliding, the net rate of lateral motion is zero due to symmetry and becomes nonzero and positive in the direction of sliding.

Previous models of velocity-dependent, multibond wear—though conceptually similar—have notable differences compared to the model proposed here.[23] For example, one stochastic model only considered the effect of the applied normal load on the bonding rate, without regard for how load may bias the reverse unbonding reaction. In that case, the bond lifetimes are independent of normal load. The model proposed here distributes the work from the normal load equally between the bonding and unbonding rates, so that bonded species are bound to the tip for longer times with increasing normal load. Additionally, the previous model restricted unbonding and wear to the same reaction coordinate, such that lateral load biases both wear and unbonding rates. Here we assume the other extreme, in which only the wear rate is impacted by velocity driven work, while unbonding is independent of velocity. In general, reality is likely somewhere in between these two extremes in which both wear and unbonding are driven by lateral force, albeit not necessarily in an identical way. Nevertheless, the model proposed here provides an explicit link between the wear rate and the bond lifetime, where the time over which the wear reaction might proceed is determined by the lifetime of the bond. Within the lifetime of a single bond, the tip can apply a maximum lateral force of $sU\tau$. The present framework thus allows the normal load to determine the bond population and bond lifetime, while the lateral motion determines the wear rate, linked to the normal load through the bond lifetime. Finally, the wear rate in the previous model is not zero in the absence of a lateral load, implying that wear would proceed in the absence of any actual sliding. Our model treats wear as a biased surface diffusion phenomenon, in which no wear occurs in the absence of sliding.

For the case of functionalized graphene, the wear rate of the functional groups from the carbon sheet depends on the surface concentration of functional groups, where the total numbers of bonded and unbonded species at initial time zero are $N_b(t=0)$ = 0 and $N_u(t=0) = \phi\pi a^2/\lambda^2$, with $\phi$ representing the relative fraction of graphene carbon atoms that are occupied by functional groups. The total number of reactive species is related to the local surface concentration through integration over the entire contact area (eq 8).

$$N = \int_0^a n(\vec{r}, t)\, d\vec{r} \tag{8}$$

The rate of change in bonded $n_b$ and unbonded $n_u$ surface concentrations is then given by eqs 9 and 10

$$\frac{dn_b(\vec{r}, t)}{dt} = k_{on}n_u(\vec{r}, t) - k_{off}n_b(\vec{r}, t) - k_w n_b(\vec{r}, t) \tag{9}$$

$$\frac{dn_u(\vec{r}, t)}{dt} = k_{off}n_b(\vec{r}, t) - k_{on}n_u(\vec{r}, t) \tag{10}$$

which account for the spatial variation of pressure within the contact over time. In general, removal of reactants need not be first order, although for simplicity we assume a first order reaction for the wear process. The total number of functional groups in the contact at any given time is then given by the integration of the concentration field within the contact. Within this proposed framework the primary unknowns are $E_{on}$, $E_{off}$, $E_w$, $\Delta V_1$, $s$, and $k_0$ (see the Methods section for a discussion of how the additional parameters are selected).

**2.2. Molecular Dynamics.** The fully atomistic model consisted of a silicon oxide block on top placed on a bilayer graphene with top layer graphene passivated with oxygen atoms. The graphene substrate had dimensions of 2 × 2 nm$^2$; the bottom layer of graphene was treated as a fixed rigid body, and one end of the top layer of graphene was also fixed. A model amorphous silicon oxide block had dimensions of 3 × 2 × 1 nm$^3$; the topmost atoms in the block were treated as a rigid body under a constant load and slid at a constant speed. A reactive force field (ReaxFF) was applied to the atoms in the model.[24−26] A Langevin thermostat was applied to the free atoms maintained a temperature of 300 K. The simulations were performed by using LAMMPS simulation software.[27]

**2.3. AFM Experiments.** All atomic force microscopy (AFM) experiments were performed with an Asylum Research MFP 3D in ambient mode conditions. The tip material was silicon, and the sample was 1−5 layers of graphene oxide (GO) obtained by spin-coating GO/water (1 mg/mL) solution on a silicon substrate. The AFM probe was a silicon tip (HQ:CSC17/AL BS, $k$ = 0.2 N/m). All measurements were done in a closed cell with a continuous dry nitrogen purge, immediately after spin-coating and drying. Pull-off force (POF) measurements were obtained from the retraction half of force−deflection curves performed as a function of normal force and sample temperatures. Wear of graphene oxide was measured as a function of sliding velocity by our two step-routine to measure relative friction (see Movie S1 and the Supporting Information). Wear was initiated by a "Drive Scan" (line scan with 0° scan angle), and the resulting wear was measured by a "Measure Scan" (rectangular scan with 90° scan angle). The friction of the line scan relative to the adjacent unmodified area gave us a "Relative Friction" datum. Relative Friction has been shown to correlate linearly to surface chemical composition on functionalized graphene by previous AFM experiments. By ramping the sliding velocity after each iteration of the two-step routine, wear on graphene oxide was explored for a wide range of velocities between 10 nm/s and 12 μm/s.


https://dx.doi.org/10.1021/acs.jpcc.0c09191
J. Phys. Chem. C 2021, 125, 4139−4145

## 3. RESULTS

**3.1. Effect of Normal Force.** In the absence of sliding, eq 9 can be used with eqs 1 and 2 to experimentally estimate the values of $E_{on}$, $E_{off}$, $k_0$, and $\Delta V_1$. Because there is no lateral force in the absence of sliding, we propose that measurements of the force required to separate the tip from the surface (the pull-off force) is linearly related to the concentration of surface bonds in the interface, making it possible to measure the net rate of bond formation as a function of applied load and temperature over time. First, we measure the relative amount of force required to separate a single asperity from a graphene oxide contact as a function of tip dwell time for various ambient temperatures between 30 and 60 °C (Figure 2A) (see the Supporting Information for non-normalized pull-off force data). The Figure 2A inset plots the logarithm of $k$ obtained from each curve as a function of $1/T$ to obtain the energy barrier. The results of the fitting were $E_{on} = 0.79 \pm 0.15$ eV, $E_{off} = 0.53 \pm 0.19$ eV, and $k_0 = 3 \times 10^{12\pm2}$ (using 80% confidence). In general, the pull-off-force data were better fit by using a power law function, consistent with previous investigations of rate−state friction of single nanoasperities with chemical reactivity at the interface, although it does not significantly alter the numerical estimation of the energy barriers.[28] In addition, we experimentally estimate the activation volume $\Delta V_1$ by measuring the single asperity pull-off force as a function of both tip dwell time and applied normal load (Figure 2B). An activation volume of $\Delta V_1 = 30 \pm 15$ Å$^3$ was found, which is consistent with previous experimental estimations of activation volumes for wear of graphene oxide.

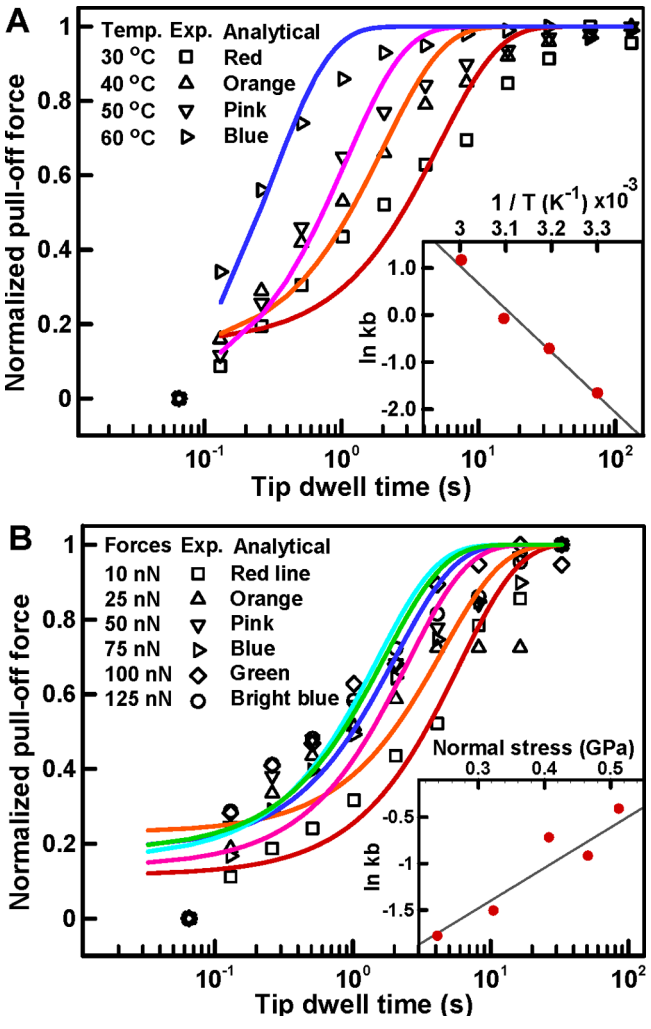


**Figure 2.** (A) Normalized pull-off-force measurements for an AFM tip on graphene oxide as a function of tip dwell time (0.1−120 s) and surface temperature (30−60 °C). The inset shows a plot of $k$ obtained from each curve as a function $T$ to obtain the energy barrier. (B) Normalized pull-off-force measurements as a function of tip dwell time and applied normal load (10−125 nN). Data are fit by using least-squares regression of eqs 9 and 10 with $U = 0$. The slopes and intercepts of the resultant rates from (A, B) are used to estimate $E_{on}$, $E_{off}$, $E_w$, and $\Delta V_1$ with 80% confidence.

**3.2. Monitoring Surface Chemical Composition during AFM Experiments.** To investigate the effect of tip velocity on sliding wear, we utilize measurable changes in surface friction to relate an immediately measurable quantity—tip friction force—to the desired parameter surface concentration. Previous studies have shown that tip friction force depends significantly on the concentration of functional groups on graphene, where a linear relationship between the two is reasonable.[21] We propose that the relative friction difference between functionalized and pristine graphene is linearly related to the surface concentration of functional groups, meaning measurements of relative friction can be used as a proxy for surface concentration. We have previously shown using ex-situ spectroscopic studies that the relative friction signal, which is the friction of the modified region with respect to the unmodified surrounding region, is linearly proportional to the concentration of functional groups on graphene and is robust to chemical changes the tip undergoes throughout an experiment. In addition, any catastrophic tear of graphene film can be immediately identified by our experiments ensuring just the removal of the oxygen molecule.[21,22] Although the simplest way to measure velocity effects is to measure wear over time for a range of constant velocities in a sequential fashion, the time required for an individual experiment significantly restricts the range of reasonable velocities that can be accessed, particularly for velocities below 1 $\mu$m/s. To expand the range of velocities available to study wear rates, we employ an experimental protocol in which the velocity is linearly increased by some constant rate between each single tip scan on the surface, allowing us to condense the experiment to a single reaction curve. Thus, it is possible to measure reaction rates for a velocity range spanning 4 orders of magnitude (see the Methods section for details of the experimental design).

**3.3. Effect of Lateral Force Induced by a Sliding Tip.** To determine the impact of velocity on wear rate, we employed AFM line scan experiments while linearly ramping tip velocity between 0.01 and 20 $\mu$m/s in 0.01 $\mu$m/s increments between each single line scan. After each line scan, we measure the friction difference between the scanned region and surrounding unscanned region. Figure 3A shows the experimental results for a range of applied normal forces between 15 and 300 nN. The results show that at low loads wear is accelerated by velocity. For example, at 15 nN we observe little wear below a velocity of 6 $\mu$m/s, and this wear accelerates dramatically above this point. In addition, as normal load on the tip increases, the velocity required to drive wear decreases. It is worth noting that there is a nonconstant minimum relative friction ratio as a function of sliding speed, denoted by the solid yellow line in Figure 3A. This trend is consistent with previous studies that show a logarithmic velocity dependence of friction between an AFM tip and a surface where no bond scission or formation occurs (noting that the division of two logarithms with differently scaled inputs is also a logarithmic function).[9,19] To ensure that this relative


https://dx.doi.org/10.1021/acs.jpcc.0c09191
J. Phys. Chem. C 2021, 125, 4139−4145

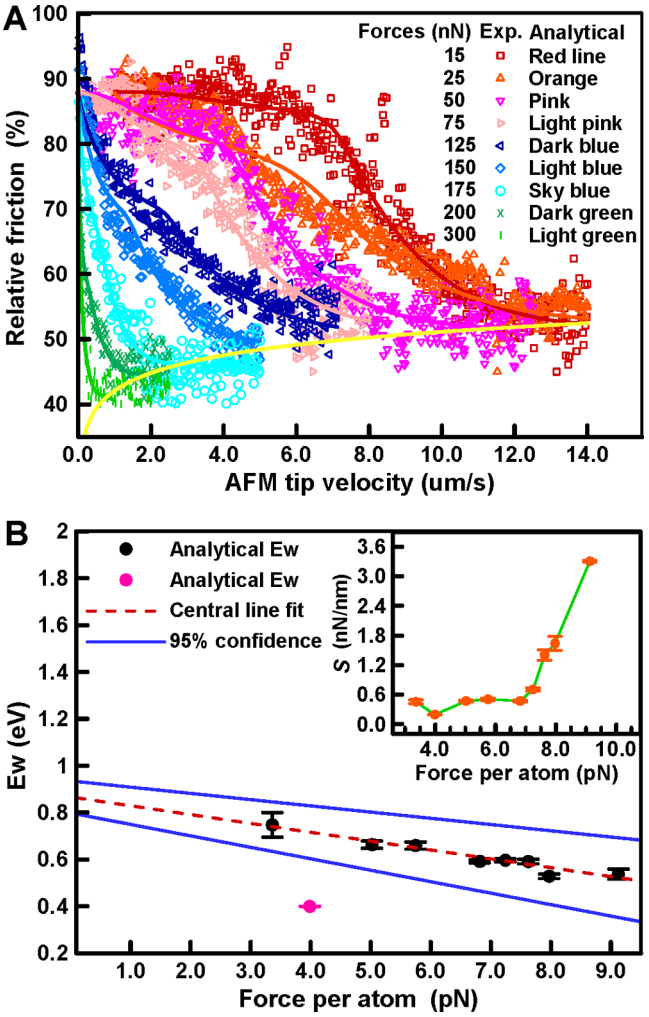


**Figure 3.** (A) Relative friction between the AFM wear track and the surrounding surface during linear tip velocity ramps for applied forces between 15 and 300 nN (experimental data points). The data are fit with least-squares regression of the numerical solutions to eqs 9 and 10 with scan histories matching experiment (solid lines). The solid yellow line represents the logarithmic dependence of the ratio of friction with speed both a reduced graphene oxide surface and pristine graphene oxide surface. (B) Resultant $E_w$ and $s$ (inset) as a function of average force per surface atom calculated by assuming the total applied force is distributed equally to each graphene atom in the tip contact. Also shown is a linear fit to the energy barrier and 95% confidence intervals. The $E_w$ at 4 pN is excluded from the fit, as the uncertainty in the fit was larger than 200%.

friction floor—which is not part of the observed wear process—does not influence our regression, we subtract the yellow line from the data during fitting. We fit the numerical solutions of eqs 9 and 10 to each velocity ramp via least-squares regression with $E_w$ and $s$ as fitting parameters. Both $E_w$ and $s$ are plotted as a function of the average force per atom on the graphene surface (calculated by dividing the total force by the estimated number of carbon atoms in the contact) in Figure 3B. The energy barrier for wear extrapolated to zero applied load is $E_{w,0} = 0.87 \pm 0.07$ eV. Between 15 and 300 nN normal load, the energy barrier follows a linear relationship $E_w = E_{w,0} - P_{ave}\Delta V_2$ where $\Delta V_2 = 3 \pm 4$ Å$^3$. Although the mechanism for a shrinking barrier for wear with increasing load is unclear, we hypothesize that larger loads would likely work to flatten out the sp$^3$ bond of the functional group on graphene, making it less stable and more susceptible to wear. Finally, the parameter $s$, which represents the stiffness of the energy barrier to wear, is $s = 0.47$ N/m at low and moderate loads and begins to increase exponentially at higher loads. This value is somewhat lower than those typically found for covalent bonds (~1 N/m). Perhaps most notably, wear in this system occurs at average atomic forces 2−3 orders of magnitude below those typically required to break covalent bonds within the time of the experiments.

## 4. DISCUSSION

**4.1. Mechanism of Atomic Scale Wear.** These results run counter to many descriptions of atomic scale wear in the literature, where the moving asperity binds to the surface atom, breaks the bonds between the atom and substrate, and carries the atom away.[5] Here, the applied atomic forces are too low to irreversibly cleave molecules from the surface. Instead, we propose that wear in this system is driven largely by thermal energy, in which the relatively gentle interactions with the sliding tip slightly bias the probability to hop in the direction of motion. This description of wear requires that wear be a dynamic process, whereby a series of highly active reversible reactions driven primarily by thermal energy are slightly perturbed and biased by interfacial loads and sliding direction.

To understand the nature of atomic scale wear in this material system, we perform molecular dynamics simulations of the wear process using REAXFF in LAMMPS (Figure 4) (see additional details in the Methods section). The interface consists of a sliding silicon oxide slab on top and bilayer graphene on the bottom. The bottom layer of graphene is rigidly fixed in space, while the top layer of graphene is rigidly supported at one end. This configuration allows the graphene to undergo lateral strain during sliding. Before the initiation of sliding, oxygen is introduced into the graphene−silicon system and allowed to adsorb onto both surfaces, with any extra free oxygen removed after the surfaces reach equilibrium. The velocity of the oxygen atoms initially chemisorbed to graphene is monitored over time. Figure 4B−D shows histograms of the oxygen atom velocities for four snapshots in time for contact forces of 1.28 and 3.2 nN. At short times, the higher loading results in more significant lateral motion of the oxygen atoms. At long times, the oxygen atoms comprise two distinct populations: (1) those moving with the silicon oxide and (2) those attached to graphene. The median velocity of each snapshot in time for contact forces of 1.28, 1.6, 2.4, and 3.2 nN is shown in Figure 4E, showing a nonlinear increase in median velocity over time, which increases more quickly with increasing load.

The equilibrium population of atoms transferred to the silicon oxide surface was 75% for the 1.28 nN load and increased to 80% for the 3.2 nN load. These results are consistent with the following behaviors predicted by our model: (1) the rate of bonding in the interface increases with increasing normal load, (2) the equilibrium population of bonded atoms to the silicon increases with increasing normal load, and (3) the bonding rate follows a first order (or higher) rate law. Interestingly, the bonding process did not largely proceed until sliding began, indicating that the quality of the contact is low initially and improves during sliding, consistent with previous simulations for graphene friction.

**4.2. Rationalizing Other Wear Behavior Types.** We further explore how wear might behave outside of our experimental sample space by plotting the instantaneous wear rate (eq 7) for the case of a fully functionalized surface as a function of both applied normal load and tip speed (Figure 5).


https://dx.doi.org/10.1021/acs.jpcc.0c09191
J. Phys. Chem. C 2021, 125, 4139−4145

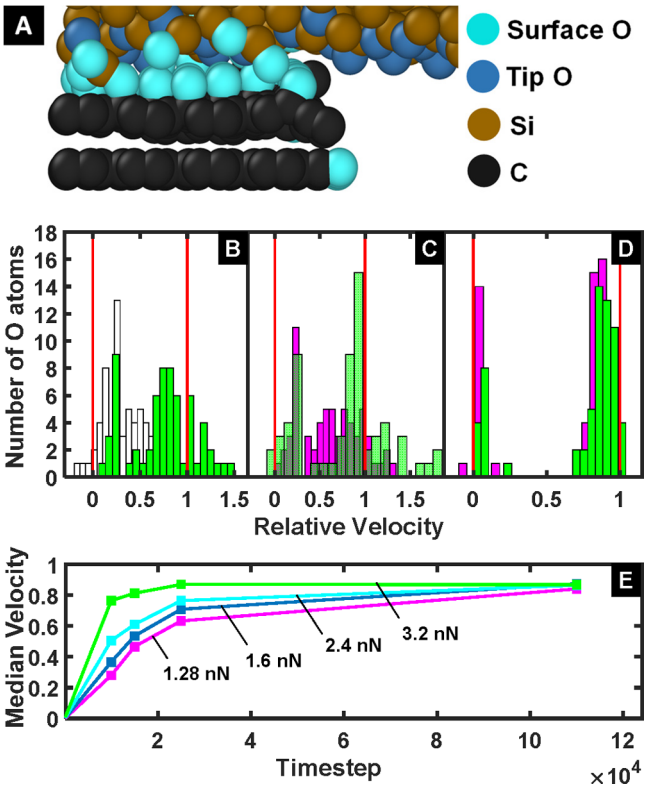


**Figure 4.** (A) A molecular dynamics simulation of a sliding slab of silicon oxide along graphene oxide, where the geometry allows for in plane strain within the graphene sheet. Black, orange, dark blue, and light blue spheres represent carbon, silicon, tip bound oxygen molecules, and surface bound molecules, respectively. (B–D) Histograms of the velocity (relative to the silicon oxide slab velocity) of each oxygen atom originally attached to the graphene sheet at timesteps of 10000, 15000, 25000, and 110000. The histogram color depicts the normal load applied to the interface (magenta = 1.28 nN; green = 3.2 nN). (E) The median relative velocity of the oxygen atoms as a function of the MD simulation timestep, showing enhanced transport at higher loads.

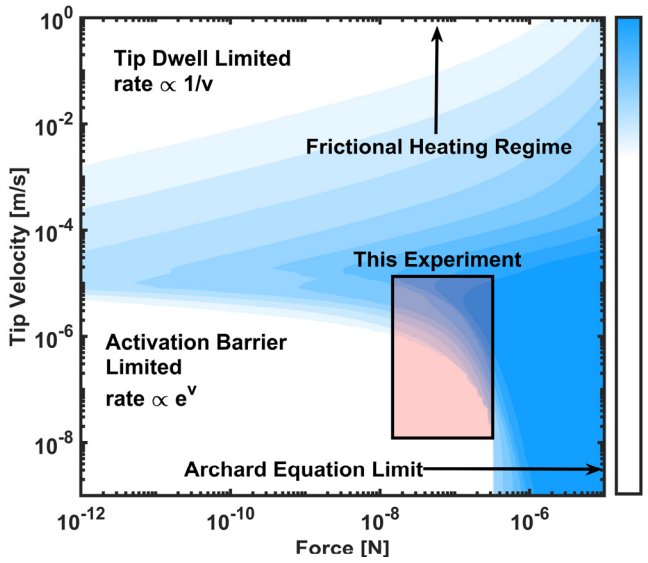


**Figure 5.** Calculated wear rates for a sliding tip on graphene oxide by using the conditions determined from experiment (red box). For all velocities, wear is exponentially activated by applied force. At low forces and tip velocities, the wear rate is an activated process for velocity. At low forces and high velocities, wear is limited by the time that a tip interacts with specific locations on the surface. At high enough forces, wear is barrierless and independent of velocity, consistent with the Archard equation. At high enough velocities, frictional heating should begin to increase wear rates (not simulated here).

At all velocities, the wear rate is a monotonically increasing function of applied load. At very large load, the barriers for both bonding and wear disappear, resulting in an Archard-type wear rate independent of velocity, although it should be noted that at these loads it is likely that more catastrophic forms of wear (which are also independent of speed) would begin to dominate. For low and moderate loads and velocities, the wear rate is an activated process that depends exponentially on load. As velocity increases, wear becomes barrierless, and the wear rate is then limited by the bonding rate, which is proportional to the tip dwell time at any given point (inversely proportional to the tip velocity). Previous works have identified experimental systems that exhibit barrierless wear. This work extends this concept to include thermally activated wear and experimentally verifies the model for the wear of graphene oxide by an AFM tip. In addition, some of the force dependent behavior is consistent with MD simulations. Velocity dependent behavior was less clear from the MD simulations, as the accessible velocities are well above the activation velocity, and the mirror boundary condition does not link tip dwell time to tip velocity. This dynamic picture of atomic scale wear as a generally reversible interfacial reaction expands our basic understanding of how wear behaves at small scales and suggests additional strategies to modulate wear through the interplay of reaction rates and sliding speed.

## 5. CONCLUSIONS

In summary, we have demonstrated that atomic scale wear is a thermally activated process driven by the lateral forces generated by the velocity of the sliding tip. A key concept behind the framework proposed here is the dynamic, reversible nature of atomic bonding and lattice site hopping within the contact, in which wear is initiated not by mechanically breaking molecular bonds but through mild bias of thermally driven reaction rates. The model is also consistent with previous measurements of nanoscale wear in which the tip dwell rate was the limiting rate factor. The model further predicts a velocity independent wear rate at high loads, consistent with more aggressive wear rates observed in macroscale experiments. Linking atomic scale transport phenomena to wear of a single nanoasperity is a key step in the grand challenge of predicting macroscale, multi-asperity wear from atomic scale forces.

## ■ ASSOCIATED CONTENT

### Supporting Information

The Supporting Information is available free of charge at https://pubs.acs.org/doi/10.1021/acs.jpcc.0c09191.

Experimental setup, pull-off-force (POF) measurements, two-step routine to monitor chemical change, tip radius measurement, and film tear (PDF)

Movie S1: automated velocity ramp experiments (MP4)

Movie S2: experiment animation (MP4)



https://dx.doi.org/10.1021/acs.jpcc.0c09191
J. Phys. Chem. C 2021, 125, 4139–4145

## AUTHOR INFORMATION


### Corresponding Author

**Jonathan R. Felts** − *Advanced NanoManufacturing Lab, J. Mike Walker '66 Department of Mechanical Engineering, Texas A&M University, College Station, Texas 77843, United States;* orcid.org/0000-0002-8232-4660; Email: jonathan.felts@tamu.edu

### Authors

**Shivaranjan Raghuraman** − *Advanced NanoManufacturing Lab, J. Mike Walker '66 Department of Mechanical Engineering, Texas A&M University, College Station, Texas 77843, United States*

**Perawat Boonpuek** − *Advanced NanoManufacturing Lab, J. Mike Walker '66 Department of Mechanical Engineering, Texas A&M University, College Station, Texas 77843, United States*

**Kyle H. King** − *Advanced NanoManufacturing Lab, J. Mike Walker '66 Department of Mechanical Engineering, Texas A&M University, College Station, Texas 77843, United States*

**Zhijiang Ye** − *Mechanical and Manufacturing Engineering, Miami University, Oxford, Ohio 45056, United States*

Complete contact information is available at: https://pubs.acs.org/10.1021/acs.jpcc.0c09191


### Notes

The authors declare no competing financial interest.

## ACKNOWLEDGMENTS

This material is based upon work supported by the National Science Foundation under Grant DMR-1848309. We thank Dr. James D. Batteas and Dr. Ali Erdemir for their valuable discussions.

## REFERENCES


(1) Holmberg, K.; Andersson, P.; Erdemir, A. Global Energy Consumption Due to Friction in Passenger Cars. *Tribol. Int.* **2012**, *47*, 221−234.

(2) Holmberg, K.; Erdemir, A. Influence of Tribology on Global Energy Consumption, Costs and Emissions. *Friction* **2017**, *5*, 263−284.

(3) Archard, J. F. Contact and Rubbing of Flat Surfaces. *J. Appl. Phys.* **1953**, *24*, 981−988.

(4) Zmitrowicz, A. Wear Patterns and Laws of Wear@ a Review. *J. Theor. Appl. Mech.* **2006**, *44*, 219−253.

(5) Jacobs, T. D.; Carpick, R. W. Nanoscale Wear as a Stress-Assisted Chemical Reaction. *Nat. Nanotechnol.* **2013**, *8*, 108−112.

(6) Rupert, T. J.; Schuh, C. A. Sliding Wear of Nanocrystalline Ni-W: Structural Evolution and the Apparent Breakdown of Archard Scaling. *Acta Mater.* **2010**, *58*, 4137−4148.

(7) Müser, M. H. Velocity Dependence of Kinetic Friction in the Prandtl-Tomlinson Model. *Phys. Rev. B: Condens. Matter Mater. Phys.* **2011**, *84*, 125419.

(8) Popov, V. L.; Gray, J. Prandtl-Tomlinson Model: History and Applications in Friction, Plasticity, and Nanotechnologies. *Z. Angew. Math. Mech.* **2012**, *92*, 683−708.

(9) Riedo, E.; Gnecco, E.; Bennewitz, R.; Meyer, E.; Brune, H. Interaction Potential and Hopping Dynamics Governing Sliding Friction. *Phys. Rev. Lett.* **2003**, *91*, 084502.

(10) Gosvami, N. N.; Feldmann, M.; Peguiron, J.; Moseler, M.; Schirmeisen, A.; Bennewitz, R. Ageing of a Microscopic Sliding Gold Contact at Low Temperatures. *Phys. Rev. Lett.* **2011**, *107*, 144303.

(11) Li, Q.; Tullis, T. E.; Goldsby, D.; Carpick, R. W. Frictional Ageing from Interfacial Bonding and the Origins of Rate and State Friction. *Nature* **2011**, *480*, 233−236.

(12) Gosvami, N.; Bares, J.; Mangolini, F.; Konicek, A.; Yablon, D.; Carpick, R. Mechanisms of Antiwear Tribofilm Growth Revealed in Situ by Single-Asperity Sliding Contacts. *Science* **2015**, *348*, 102−106.

(13) Zheng, X.; Gao, L.; Yao, Q.; Li, Q.; Zhang, M.; Xie, X.; Qiao, S.; Wang, G.; Ma, T.; Di, Z.; Luo, J.; Wang, X. Robust Ultra-Low-Friction State of Graphene Via Moiré Superlattice Confinement. *Nat. Commun.* **2016**, *7*, 1−7.

(14) Chen, L.; He, H.; Wang, X.; Kim, S. H.; Qian, L. Tribology of Si/$SiO_2$ in Humid Air: Transition from Severe Chemical Wear to Wearless Behavior at Nanoscale. *Langmuir* **2015**, *31*, 149−156.

(15) Chen, L.; Qi, Y.; Yu, B.; Qian, L. Sliding Speed-Dependent Tribochemical Wear of Oxide-Free Silicon. *Nanoscale Res. Lett.* **2017**, *12*, 404.

(16) He, H.; Xiao, T.; Qiao, Q.; Yu, J.; Zhang, Y. Contrasting Roles of Speed on Wear of Soda Lime Silica Glass in Dry and Humid Air. *J. Non-Cryst. Solids* **2018**, *502*, 236−243.

(17) He, H.; Yang, L.; Yu, J.; Zhang, Y.; Qi, H. Velocity-Dependent Wear Behavior of Phosphate Laser Glass. *Ceram. Int.* **2019**, *45*, 19777.

(18) Degiampietro, K.; Colaco, R. Nanoabrasive Wear Induced by an Afm Diamond Tip on Stainless Steel. *Wear* **2007**, *263*, 1579−1584.

(19) Bhushan, B.; Kwak, K. J. Velocity Dependence of Nanoscale Wear in Atomic Force Microscopy. *Appl. Phys. Lett.* **2007**, *91*, 163113.

(20) Jiang, J.; Arnell, R. D. The Effect of Sliding Speed on Wear of Diamond-Like Carbon Coatings. *Wear* **1998**, *218*, 223−231.

(21) Felts, J. R.; Oyer, A. J.; Hernández, S. C.; Whitener Jr, K. E.; Robinson, J. T.; Walton, S. G.; Sheehan, P. E. Direct Mechanochemical Cleavage of Functional Groups from Graphene. *Nat. Commun.* **2015**, *6*, 6467.

(22) Raghuraman, S.; Elinski, M. B.; Batteas, J. D.; Felts, J. R. Driving Surface Chemistry at the Nanometer Scale Using Localized Heat and Stress. *Nano Lett.* **2017**, *17*, 2111−2117.

(23) Shao, Y.; Jacobs, T. D. B.; Jiang, Y.; Turner, K. T.; Carpick, R. W.; Falk, M. L. Multibond Model of Single-Asperity Tribochemical Wear at the Nanoscale. *ACS Appl. Mater. Interfaces* **2017**, *9*, 35333−35340.

(24) Ponomarev, I.; van Duin, A. C. T.; Kroll, P. Reactive Force Field for Simulations of the Pyrolysis of Polysiloxanes into Silicon Oxycarbide Ceramics. *J. Phys. Chem. C* **2019**, *123*, 16804−16812.

(25) Soria, F. A.; Zhang, W.; Paredes-Olivera, P. A.; van Duin, A. C. T.; Patrito, E. M. Si/C/H Reaxff Reactive Potential for Silicon Surfaces Grafted with Organic Molecules. *J. Phys. Chem. C* **2018**, *122*, 23515−23527.

(26) Soria, F. A.; Zhang, W.; van Duin, A. C. T.; Patrito, E. M. Thermal Stability of Organic Monolayers Grafted to Si(111): Insights from Reaxff Reactive Molecular Dynamics Simulations. *ACS Appl. Mater. Interfaces* **2017**, *9*, 30969−30981.

(27) Plimpton, S. Fast Parallel Algorithms for Short-Range Molecular Dynamics. *J. Comput. Phys.* **1995**, *117*, 1.

(28) Tian, K.; Gosvami, N. N.; Goldsby, D. L.; Liu, Y.; Szlufarska, I.; Carpick, R. W. Load and Time Dependence of Interfacial Chemical Bond-Induced Friction at the Nanoscale. *Phys. Rev. Lett.* **2017**, *118*, 076103.